Eur. Phys. J. C 50, 363–371 (2007)
DOI 10.1140/epjc/s10052-007-0209-7

THE EUROPEAN PHYSICAL JOURNAL C

Regular Article – Theoretical Physics

Branching ratio and CP-asymmetry of $B_s \to \rho(\omega)K$ decays in the perturbative QCD approach

Zhen-Jun Xiao[a], Xin-Fen Chen, Dong-Qin Guo

Department of Physics and Institute of Theoretical Physics, Nanjing Normal University, Nanjing, Jiangsu 210097, P.R. China

Received: 20 September 2006 / Revised version: 20 December 2006 /
Published online: 3 February 2007 –

Abstract. In this paper, we calculate the branching ratios and CP-violating asymmetries for $B_s \to \rho^{\pm}K^{\mp}$, $\rho^0\bar{K}^0$ and $\omega\bar{K}^0$ decays in the perturbative QCD factorization approach. The theoretical predictions for the CP-averaged branching ratios of the considered decays are $\mathrm{Br}(B_s \to \rho^{\pm}K^{\mp}) \approx 24.7 \times 10^{-6}$, $\mathrm{Br}(B_s \to \rho^0\bar{K}^0) \approx 1.2 \times 10^{-7}$ and $\mathrm{Br}(B_s \to \omega\bar{K}^0) \approx 1.7 \times 10^{-7}$; and we also predict large CP-violating asymmetries for the considered decay modes. Specifically, the large $A_{CP}^{\mathrm{dir}}(B_s \to \rho^{\pm}K^{\mp})$ at -12% level plus large branching ratio at 10^{-5} level are measurable in the forthcoming LHC-b experiments.

PACS. 13.25.Hw; 12.38.Bx; 14.40.Nd

1 Introduction

Charmless B meson decay is a good place to test the standard model (SM), study CP-violation and look for a signal or evidence of possible new physics beyond the SM. Since 1999, many such decay modes have been observed in the B factory experiments. In the forthcoming Large Hadron Collider beauty (LHC-b) experiments, a large number of heavier B_s and B_c mesons together with light $B_{u,d}$ mesons will be produced [1]. The study of the charmless decays of B_s meson is therefore becoming more interesting than ever before [2–4].

By employing the generalized factorization approach [5–10] or the QCD factorization (QCDF) approach [11, 12], about 40 $B_s \to h_1h_2$ (h_i stands for the light pseudo-scalar or vector mesons) decay modes have been studied in the framework of SM [13–16] or in some new physics models beyond the SM [17]. In [18–22], the branching ratios and CP-violating asymmetries of $B_s \to \pi^+\pi^-$, $\pi\rho$, πK, $\rho(\omega)K^*$ and $\pi\eta^{(\prime)}$ decays have been calculated by employing the perturbative QCD (pQCD) factorization approach [23–30]. Motivated by the expected success in LHC-b experiments and other hadronic B meson experiments, we here continue the investigation of more charmless B_s decays in the pQCD factorization approach.

In this paper, we will study the $B_s \to \rho^{\pm}K^{\mp}$, $\rho^0\bar{K}^0$ and $\omega\bar{K}^0$ decays in the pQCD approach. In principle, the physics for the B_s two-body hadronic decays is very similar to that for the B_d meson, except that the spectator d quark is replaced by the s quark.

For $B_s \to \rho(\omega)K$ decays, the B_s meson is heavy, setting at rest and decaying into two light mesons (i.e. $\rho(\omega)$ and K) with large momenta. Therefore the light final state mesons are moving very fast in the rest frame of the B_s meson. In this case, the short distance hard process dominates the decay amplitude. We assume that the soft final state interaction is not important for such decays, since there is not enough time for light mesons to exchange soft gluons. Therefore, it makes the pQCD reliable in calculating the $B_s \to \rho(\omega)K$ decays. With the Sudakov resummation, we can include the leading double logarithms for all loop diagrams, in association with the soft contribution.

This paper is organized as follows. In Sect. 2, we give a brief review for the pQCD factorization approach. In Sect. 3, we calculate analytically the related Feynman diagrams and present the decay amplitudes for the studied decay modes. In Sect. 4, we show the numerical results for the branching ratios and CP-asymmetries of $B_s \to \rho(\omega)K$ decays, comparing them with the results obtained in the QCDF approach. The summary and some discussions are included in the final section.

2 Theoretical framework

The three scale pQCD factorization approach has been developed and applied in the non-leptonic $B_{(s)}$ meson decays since some time ago [25–30]. In this approach, the decay amplitude is separated into soft (Φ), hard (H), and harder (C) dynamics, characterized by different energy scales (t, m_b, M_W). It is conceptually written as the

[a] e-mail: xiaozhenjun@njnu.edu.cn

convolution:

$$\mathcal{A}(B_{(s)} \to M_1 M_2) \sim \int \mathrm{d}^4k_1\,\mathrm{d}^4k_2\,\mathrm{d}^4k_3 \times \mathrm{Tr}[C(t)\Phi_{B_{(s)}}(k_1)\Phi_{M_1}(k_2)\Phi_{M_2}(k_3)H(k_1,k_2,k_3,t)]\,, \quad (1)$$

where the k_i are the momenta of the light quarks included in each of the mesons, and the term "Tr" denotes the trace over Dirac and color indices. The harder dynamic involves the four quark operators described by the Wilson coefficient $C(t)$. The function $H(k_1,k_2,k_3,t)$ describes the four quark operator and the spectator quark connected by a hard gluon whose scale is at the order of $M_{B_{(s)}}$, so that this hard part H can be perturbatively calculated. The soft dynamics is factorized into the meson wave function Φ_M, which describes hadronization of the quark and anti-quark pair into the meson M. While the function H depends on the processes considered, the wave function Φ_M is independent of the specific processes. Using the wave functions determined from other well measured processes, one can make quantitative predictions here.

For the B_s meson decays, since the b quark is rather heavy, we consider the B_s meson at rest for simplicity. It is convenient to use light-cone coordinate $(p^+,p^-,\mathbf{p}_\mathrm{T})$ to describe the meson's momenta. The B_s meson and the two final state meson momenta can be written as

$$P_{B_s} = \frac{M_{B_s}}{\sqrt{2}}(1,1,\mathbf{0}_\mathrm{T})\,,\quad P_{\rho(\omega)} = \frac{M_{B_s}}{\sqrt{2}}\big(1,r^2_{\rho(\omega)},\mathbf{0}_\mathrm{T}\big)\,,$$
$$P_k = \frac{M_{B_s}}{\sqrt{2}}\big(0,1-r^2_{\rho(\omega)},\mathbf{0}_\mathrm{T}\big)\,, \quad (2)$$

respectively, where $r_{\rho(\omega)} = m_{\rho(\omega)}/M_{B_s}$; the term proportional to $m_K^2/M_{B_s}^2$ has been neglected.

For the $B_s \to \rho(\omega)K$ decays considered here, only the $\rho(\omega)$ meson's longitudinal part contributes to the decays; its polar vector is $\epsilon_\mathrm{L} = \frac{M_{B_s}}{\sqrt{2}M_{\rho(\omega)}}(1,-r^2_{\rho(\omega)},\mathbf{0}_\mathrm{T})$. Putting the light (anti-) quark momenta in the B_s, $\rho(\omega)$ and K meson k_1, k_2, and k_3, respectively, we can choose

$$k_1 = \big(x_1P_1^+,0,\mathbf{k}_{1\mathrm{T}}\big)\,,\quad k_2 = \big(x_2P_2^+,0,\mathbf{k}_{2\mathrm{T}}\big)\,,$$
$$k_3 = \big(0,x_3P_3^-,\mathbf{k}_{3\mathrm{T}}\big)\,. \quad (3)$$

In the pQCD approach, we keep the transverse momentum k_T in the above expressions, in order to avoid the endpoint singularity. Then the integration over k_1^-, k_2^-, and k_3^+ in (1) will lead to

$$\mathcal{A}(B_s \to \rho(\omega)k) \sim \int \mathrm{d}x_1\,\mathrm{d}x_2\,\mathrm{d}x_3 b_1\,\mathrm{d}b_1 b_2\,\mathrm{d}b_2 b_3\,\mathrm{d}b_3 \times \mathrm{Tr}\big[C(t)\Phi_{B_s}(x_1,b_1)\Phi_{\rho(\omega)}(x_2,b_2)\Phi_k(x_3,b_3) \times H(x_i,b_i,t)S_t(x_i)\mathrm{e}^{-S(t)}\big]\,, \quad (4)$$

where b_i is the conjugate space coordinate of $k_{i\mathrm{T}}$, and t is the largest energy scale in the function $H(x_i,b_i,t)$. The large logarithms $(\ln m_W/t)$ coming from QCD radiative corrections to four quark operators are included in the Wilson coefficients $C(t)$. The large double logarithms $(\ln^2 x_i)$ on the longitudinal direction are summed by the threshold resummation [31], and they lead to the function $S_t(x_i)$ which smears the end-point singularities on x_i. The last term, $\mathrm{e}^{-S(t)}$, is the Sudakov form factor, resulting from overlap of soft and collinear divergences, which suppresses the soft dynamics effectively [32]. Thus, it makes the perturbative calculation of the hard part H applicable at an intermediate scale, i.e., the M_{B_s} scale. We will calculate analytically the function $H(x_i,b_i,t)$ for $B_s \to \rho(\omega)K$ decays in the first order in an α_s expansion and give the decay amplitudes in the next section.

For $B_s \to \rho(\omega)K$ decays, the weak effective Hamiltonian $\mathcal{H}_\mathrm{eff}$ can be written as [33]

$$\mathcal{H}_\mathrm{eff} = \frac{G_\mathrm{F}}{\sqrt{2}}\Bigg[V_{ub}V_{ud}^*\big(C_1(\mu)O_1^u(\mu) + C_2(\mu)O_2^u(\mu)\big) - V_{tb}V_{td}^*\sum_{i=3}^{10}C_i(\mu)O_i(\mu)\Bigg]\,. \quad (5)$$

We specify below the operators in $\mathcal{H}_\mathrm{eff}$ for the $b \to d$ transition:

$$\begin{aligned}
O_1^u &= \bar{d}_\alpha\gamma^\mu Lu_\beta\cdot\bar{u}_\beta\gamma_\mu Lb_\alpha\,,\\
O_2^u &= \bar{d}_\alpha\gamma^\mu Lu_\alpha\cdot\bar{u}_\beta\gamma_\mu Lb_\beta\,,\\
O_3 &= \bar{d}_\alpha\gamma^\mu Lb_\alpha\cdot\sum_{q'}\bar{q}'_\beta\gamma_\mu Lq'_\beta\,,\\
O_4 &= \bar{d}_\alpha\gamma^\mu Lb_\beta\cdot\sum_{q'}\bar{q}'_\beta\gamma_\mu Lq'_\alpha\,,\\
O_5 &= \bar{d}_\alpha\gamma^\mu Lb_\alpha\cdot\sum_{q'}\bar{q}'_\beta\gamma_\mu Rq'_\beta\,,\\
O_6 &= \bar{d}_\alpha\gamma^\mu Lb_\beta\cdot\sum_{q'}\bar{q}'_\beta\gamma_\mu Rq'_\alpha\,,\\
O_7 &= \frac{3}{2}\bar{d}_\alpha\gamma^\mu Lb_\alpha\cdot\sum_{q'}e_{q'}\bar{q}'_\beta\gamma_\mu Rq'_\beta\,,\\
O_8 &= \frac{3}{2}\bar{d}_\alpha\gamma^\mu Lb_\beta\cdot\sum_{q'}e_{q'}\bar{q}'_\beta\gamma_\mu Rq'_\alpha\,,\\
O_9 &= \frac{3}{2}\bar{d}_\alpha\gamma^\mu Lb_\alpha\cdot\sum_{q'}e_{q'}\bar{q}'_\beta\gamma_\mu Lq'_\beta\,,\\
O_{10} &= \frac{3}{2}\bar{d}_\alpha\gamma^\mu Lb_\beta\cdot\sum_{q'}e_{q'}\bar{q}'_\beta\gamma_\mu Lq'_\alpha\,, \quad (6)
\end{aligned}$$

where α and β are the $SU(3)$ color indices; L and R are the left- and right-handed projection operators with $L=(1-\gamma_5)$, $R=(1+\gamma_5)$. The sum over q' runs over the quark fields that are active at the scale $\mu = O(m_b)$. The pQCD approach works well for the leading twist approximation and leading double logarithm summation. For the Wilson coefficients $C_i(\mu)$ $(i=1,\ldots,10)$, we will also use the leading order (LO) expressions, although the next-to-leading order calculations already exists in the litera-

ture [33]. This is a consistent way to cancel the explicit μ dependence in the theoretical formulae.

For the renormalization group evolution of the Wilson coefficients from higher scale to lower scale, we use the formulae as given in [34] directly. At the high m_W scale, the leading order Wilson coefficients $C_i(M_W)$ are simple and can be found easily in [33]. In the pQCD approach, the scale t may be larger or smaller than the m_b scale. For the case of $m_b < t < m_W$, we evaluate the Wilson coefficients at the t scale using leading logarithm running equations, as given in (C1) of [34]. For the case of $t < m_b$, we then evaluate the Wilson coefficients at the t scale by using $C_i(m_b)$ as input and the formulae given in Appendix D of [34].

For the wave function of the heavy B_s meson, we take

$$\Phi_{B_s} = \frac{1}{\sqrt{2N_c}}(\not{p}_{B_s} + M_{B_s})\gamma_5 \phi_{B_s}(\mathbf{k}_1)\,. \tag{7}$$

Here only the contribution of the Lorentz structure $\phi_{B_s}(\mathbf{k}_1)$ is taken into account, since the contribution of the second Lorentz structure $\bar{\phi}_{B_s}$ is numerically small and has been neglected.

The wave function for the pseudo-scalar meson K is given by

$$\Phi_K(P,x,\zeta) \equiv \frac{\mathrm{i}}{\sqrt{2N_c}}\gamma_5\big\{\not{p}_K \phi_K^A(x) + m_0^K \phi_K^P(x) + \zeta m_0^K(\not{v}\not{n} - vn)\phi_K^T(x)\big\}\,, \tag{8}$$

where P and x are the momentum and the momentum fraction of the K meson, respectively. We assumed here that the wave function of the K meson is the same as the wave function of the π meson. The parameter ζ is either $+1$ or -1, depending on the assignment of the momentum fraction x.

For $B \to \rho K$ decay, the vector meson ρ is longitudinally polarized. The relevant longitudinal polarized component of the wave function is given by [37–39]

$$\Phi_\rho = \frac{1}{\sqrt{2N_c}}\big\{\not{\epsilon}\left[m_\rho \phi_\rho(x) + \not{p}_\rho \phi_\rho^t(x)\right] + m_\rho \phi_\rho^s(x)\big\}\,, \tag{9}$$

where the first term is the leading twist wave function (twist-2), while the second and third terms are sub-leading twist (twist-3) wave functions. For $B \to \omega K$ decay, we have an expression similar to (9).

3 Perturbative calculations

In this section, we will calculate the hard part $H(t)$ which involves the four quark operators and the necessary hard gluon connecting the four quark operator and the spectator quark. Similar to the decay $B_s \to \pi K$ [20], the eight lowest order Feynman diagrams contributing to the $B_s \to \rho K$ or ωK decays are illustrated in Fig. 1. We first calculate the usual factorizable diagrams a and b. The operators $O_{1,2}$ and $O_{3,4,9,10}$ are $(V-A)(V-A)$ currents; the sum of their

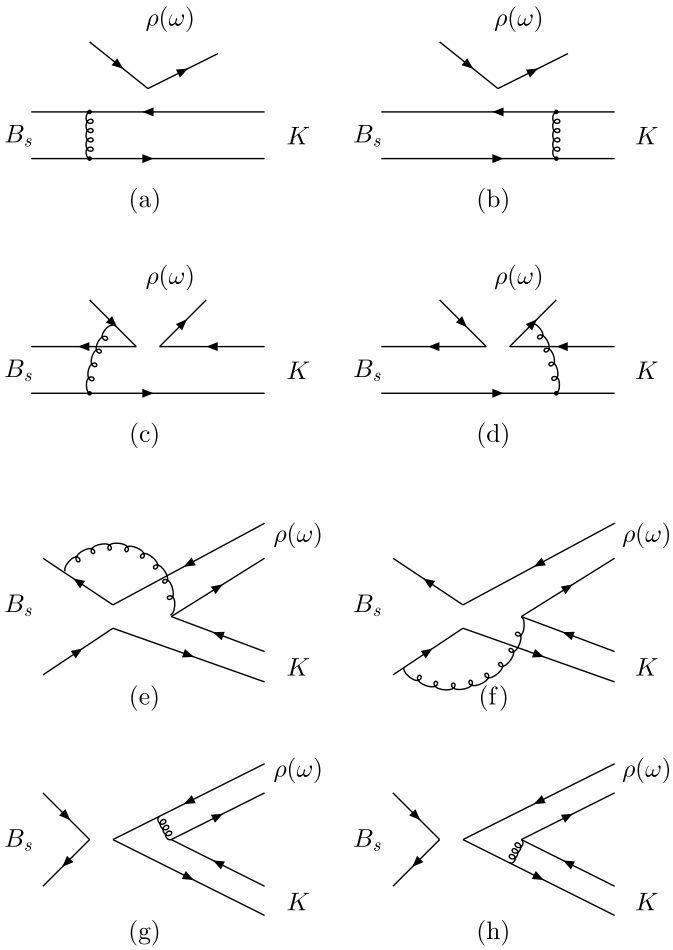

Fig. 1. Diagrams contributing to the $B_s \to \rho K$ and ωK decays (diagram **a** and **b** contribute to the $B_s \to K$ form factor $F_0^{B_s\to K}$)

amplitudes is given by

$$\begin{aligned} F_{eK} = -8\pi C_{\mathrm{F}} f_\rho M_{B_s}^4 \int_0^1 \mathrm{d}x_1\,\mathrm{d}x_3 \\ \times \int_0^\infty b_1\,\mathrm{d}b_1 b_3\,\mathrm{d}b_3 \phi_{B_s}(x_1,b_1) \\ \times \big\{\big[(2-x_3)\phi_K^A(x_3,b_3) \\ + (2x_3-1)r_K\big(\phi_K^P(x_3,b_3) - \phi_K^T(x_3,b_3)\big)\big] \\ \times \alpha_{\mathrm{s}}\big(t_e^1\big) h_e(x_1,1-x_3,b_1,b_3)\exp\big[-S_{ab}\big(t_e^1\big)\big] \\ + 2r_k\phi_K^P(x_3,b_3)\alpha_{\mathrm{s}}\big(t_e^2\big) h_e(1-x_3,x_1,b_3,b_1) \\ \times \exp\big[-S_{ab}\big(t_e^2\big)\big]\big\}\,, \end{aligned} \tag{10}$$

where $C_{\mathrm{F}} = 4/3$ is a color factor. The function h_e^i, the energy scales t_e^i and the Sudakov factors S_{ab} are displayed in the appendix. In the above equation, we do not include the Wilson coefficients of the corresponding operators, which are process dependent. They will be shown later in this section for different decay channels. The diagrams Fig. 1a and b are also the diagrams for the $B_s \to K$ form factor $F_0^{B_s\to K}$. Therefore we can extract $F_0^{B_s\to K}$ from (10).

The operators $O_{5,6,7,8}$ have the structure of $(V-A)(V+A)$. In some decay channels, some of these operators contribute to the decay amplitude in a factorizable way. Since only the axial-vector part of the $(V+A)$ current contributes to the pseudo-scalar meson production, $\langle\rho|V-A|B\rangle\langle K|V+A|0\rangle = -\langle\rho|V-A|B\rangle\langle K|V-A|0\rangle$, we find that

$$F_{eK}^{P_1} = -F_{eK}\,. \tag{11}$$

In some other cases, we need to do a Fierz transformation for these operators to get the right flavor and color structure for factorization to work. In this case, we get $(S+P)(S-P)$ operators from $(V-A)(V+A)$ ones. For the decays considered here, we find

$$F_{eK}^{P_2} = 0\,. \tag{12}$$

For the non-factorizable diagram Fig. 1c and d, all three meson wave functions are involved. The integration of b_3 can be performed using the δ function $\delta(b_3-b_1)$, leaving only integration of b_1 and b_2. For the $(V-A)(V-A)$ operators, the result is

$$\begin{aligned} M_{eK} = {} & \frac{32}{\sqrt{6}}\pi C_{\rm F} M_{B_s}^4 \int_0^1 {\rm d}x_1\,{\rm d}x_2\,{\rm d}x_3 \\ & \times \int_0^\infty b_1\,{\rm d}b_1 b_2\,{\rm d}b_2 \phi_{B_s}(x_1,b_1)\phi_\rho(x_2,b_2) \\ & \times \big\{(1-x_3)\big[\phi_K^A(x_3,b_1) + 2r_k\phi_K^T(x_3,b_1)\big] \\ & \quad \times \alpha_{\rm s}(t_f) h_f(x_1,x_2,1-x_3,b_1,b_2)\exp[-S_{cd}(t_f)]\big\}. \end{aligned} \tag{13}$$

For the $(V-A)(V+A)$ and $(S-P)(S+P)$ operators, the results are

$$\begin{aligned} M_{eK}^{P_1} = {} & \frac{64}{\sqrt{6}}\pi C_{\rm F} G_{\rm F} M_{B_s}^4 r_\rho \int_0^1 {\rm d}x_1\,{\rm d}x_2\,{\rm d}x_3 \\ & \times \int_0^\infty b_1\,{\rm d}b_1 b_2\,{\rm d}b_2 \phi_{B_s}(x_1,b_1) \\ & \times \big\{\big[x_2\phi_K^A(x_3,b_1)\big(\phi_\rho^s(x_2,b_2) - \phi_\rho^t(x_2,b_2)\big) \\ & \quad + r_K\big((1+x_2-x_3)\big(\phi_K^P(x_3,b_1)\phi_\rho^s(x_2,b_2) \\ & \qquad - \phi_K^T(x_3,b_1)\phi_\rho^t(x_2,b_2)\big) \\ & \quad + (1-x_2-x_3)\big(\phi_K^P(x_3,b_1)\phi_\rho^t(x_2,b_2) \\ & \qquad - \phi_K^T(x_3,b_1)\phi_\rho^s(x_2,b_2)\big)\big)\big] \\ & \quad \times \alpha_{\rm s}(t_f) h_f(x_1,x_2,1-x_3,b_1,b_2)\exp[-S_{cd}(t_f)]\big\}, \end{aligned} \tag{14}$$

$$M_{eK}^{P_2} = -M_{eK}\,. \tag{15}$$

For the non-factorizable annihilation diagram in Fig. 1e and f, again all three wave functions are involved. Here we have two kinds of contributions. M_{aK} is the contribution containing the operator type $(V-A)(V-A)$, while $M_{aK}^{P_1}$ is the contribution containing operator type $(V-A)(V+A)$:

$$\begin{aligned} M_{aK} = {} & \frac{32}{\sqrt{6}}\pi C_{\rm F} M_{B_s}^4 \int_0^1 {\rm d}x_1\,{\rm d}x_2\,{\rm d}x_3 \\ & \times \int_0^\infty b_1\,{\rm d}b_1 b_2\,{\rm d}b_2 \phi_{B_s}(x_1,b_1) \\ & \times \big\{\big[x_2\phi_\rho(x_2,b_2)\phi_K^A(x_3,b_2) \\ & \quad + r_\rho r_K\big((x_2-x_3)\big(\phi_K^P(x_3,b_2)\phi_\rho^t(x_2,b_2) \\ & \qquad + \phi_K^T(x_3,b_2)\phi_\rho^s(x_2,b_2)\big) \\ & \quad + (2+x2+x3)\phi_K^P(x_3,b_2)\phi_\rho^s(x_2,b_2) \\ & \quad + (-2+x_2+x_3)\phi_K^T(x_3,b_2)\phi_\rho^t(x_2,b_2)\big)\big] \\ & \quad \times \alpha_{\rm s}\big(t_f^2\big) h_f^2(x_1,x_2,x_3,b_1,b_2)\exp\big[-S_{ef}\big(t_f^2\big)\big] \\ & + \big[-x_3\phi_\rho(x_2,b_2)\phi_K^A(x_3,b_2) \\ & \quad + r_\rho r_K\big((x_2-x_3)\big(\phi_K^P(x_3,b_2)\phi_\rho^t(x_2,b_2) \\ & \qquad + \phi_K^T(x_3,b_2)\phi_\rho^s(x_2,b_2)\big) \\ & \quad - (x_2+x_3)\big(\phi_K^P(x_3,b_2)\phi_\rho^s(x_2,b_2) \\ & \qquad + \phi_K^T(x_3,b_2)\phi_\rho^t(x_2,b_2)\big)\big)\big] \\ & \quad \times \alpha_{\rm s}\big(t_f^1\big) h_f^1(x_1,x_2,x_3,b_1,b_2)\exp\big[-S_{ef}\big(t_f^1\big)\big]\big\}\,, \end{aligned} \tag{16}$$

$$\begin{aligned} M_{aK}^{P_1} = {} & \frac{32}{\sqrt{6}}\pi C_{\rm F} M_{B_s}^4 \int_0^1 {\rm d}x_1\,{\rm d}x_2\,{\rm d}x_3 \\ & \times \int_0^\infty b_1\,{\rm d}b_1 b_2\,{\rm d}b_2 \phi_{B_s}(x_1,b_1) \\ & \times \big\{\big[r_\rho(x_2-2)\phi_K^A(x_3,b_2)\big(\phi_\rho^t(x_2,b_2) + \phi_\rho^s(x_2,b_2)\big) \\ & \quad + r_K(2-x_3)\phi_\rho(x_2,b_2) \\ & \qquad \times \big(\phi_K^P(x_3,b_2) + \phi_K^T(x_3,b_2)\big)\big] \\ & \quad \times \alpha_{\rm s}\big(t_f^2\big) h_f^2(x_1,x_2,x_3,b_1,b_2)\exp\big[-S_{ef}\big(t_f^2\big)\big] \\ & + \big[r_\rho(-x_2)\phi_K^A(x_3,b_2)\big(\phi_\rho^t(x_2,b_2) + \phi_\rho^s(x_2,b_2)\big) \\ & \quad + r_K x_3\phi_\rho(x_2,b_2)\big(\phi_K^P(x_3,b_2) + \phi_K^T(x_3,b_2)\big)\big] \\ & \quad \times \alpha_{\rm s}\big(t_f^1\big) h_f^1(x_1,x_2,x_3,b_1,b_2)\exp\big[-S_{ef}\big(t_f^1\big)\big]\big\}\,, \end{aligned} \tag{17}$$

where $r_K = m_0^K/M_{B_s}$ and $r_\rho = m_\rho/M_{B_s}$.

The factorizable annihilation diagram Fig. 1g and h involve only ρ and K wave functions. There are also two kinds of decay amplitudes for these two diagrams. F_{aK} is for $(V-A)(V-A)$ type operators, and $F_{aK}^{P_2}$ is for $(S-P)(S+P)$ type operators,

$$\begin{aligned} F_{aK} = {} & 8\pi C_{\rm F} f_{B_s} M_{B_s}^4 \int_0^1 {\rm d}x_2\,{\rm d}x_3 \int_0^\infty b_2\,{\rm d}b_2 b_3\,{\rm d}b_3 \\ & \times \big\{\big[x_3\phi_\rho(x_2,b_2)\phi_K^A(x_3,b_3) + 2r_\rho r_k\phi_\rho^s(x_2,b_2) \\ & \quad \times \big((1+x_3)\phi_K^P(x_3,b_3)(x_3-1)\phi_K^T(x_3,b_3)\big)\big] \\ & \quad \times \alpha_{\rm s}\big(t_e^3\big) h_a(x_2,x_3,b_2,b_3)\exp\big[-S_{gh}\big(t_e^3\big)\big] \\ & - \big[x_2\phi_\rho(x_2,b_2)\phi_K^A(x_3,b_3) + 2r_\rho r_k\phi_K^P(x_3,b_3) \\ & \quad \times \big((1+x_2)\phi_\rho^s(x_2,b_2)(x_2-1)\phi_\rho^t(x_2,b_2)\big)\big] \\ & \quad \times \alpha_{\rm s}\big(t_e^4\big) h_a(x_3,x_2,b_3,b_2)\exp\big[-S_{gh}\big(t_e^4\big)\big]\big\}\,, \end{aligned} \tag{18}$$

$$
\begin{aligned}
F_{aK}^{P_2} = & -16\pi C_{\rm F} f_{B_s} M_{B_s}^4 \int_0^1 {\rm d}x_2\,{\rm d}x_3 \int_0^\infty b_2\,{\rm d}b_2 b_3\,{\rm d}b_3 \\
& \times \Big\{ \big[2r_\rho \phi_\rho^s(x_2,b_2)\phi_K^A(x_3,b_3) \\
& \quad + r_k x_3 \phi_\rho(x_2,b_2)\big(\phi_K^P(x_3,b_3) - \phi_K^T(x_3,b_3)\big)\big] \\
& \quad \times \alpha_{\rm s}\big(t_e^3\big) h_a(x_2,x_3,b_2,b_3) \exp\big[-S_{gh}\big(t_e^3\big)\big] \\
& + \big[x_2 r_\rho \phi_K^A(x_3,b_3)\big(\phi_\rho^s(x_2,b_2) - \phi_\rho^t(x_2,b_2)\big) \\
& \quad + 2r_k \phi_\rho(x_2,b_2)\phi_K^P(x_3,b_3)\big] \\
& \quad \times \alpha_{\rm s}\big(t_e^4\big) h_a(x_3,x_2,b_3,b_2) \exp\big[-S_{gh}\big(t_e^4\big)\big] \Big\} .
\end{aligned} \tag{19}
$$

In the above equations, we have assumed that $x_1 \ll x_2, x_3$. Since the light quark momentum fraction x_1 in the B meson is peaked at the small x_1 region, this is not a bad approximation. The numerical results also show that this approximation makes very little difference in the final result.

Combining the contributions from different diagrams, the total decay amplitude for $B_s \to \rho^+ K^-$ decay can be written as

$$
\begin{aligned}
\mathcal{M}(\rho^+ K^-) = & F_{eK}\left[\xi_u\left(\frac{1}{3}C_1 + C_2\right)\right. \\
& \left. - \xi_t\left(\frac{1}{3}C_3 + C_4 + \frac{1}{3}C_9 + C_{10}\right)\right] \\
& + M_{eK}[\xi_u C_1 - \xi_t(C_3 + C_9)] \\
& - M_{eK}^{P_1}\xi_t(C_5 + C_7) \\
& - M_{aK}\xi_t\left(C_3 - \frac{1}{2}C_9\right) - M_{aK}^{P_1}\xi_t\left(C_5 - \frac{1}{2}C_7\right) \\
& - F_{aK}\xi_t\left(\frac{1}{3}C_3 + C_4 - \frac{1}{6}C_9 - \frac{1}{2}C_{10}\right) \\
& - F_{aK}^{P_2}\xi_t\left(\frac{1}{3}C_5 + C_6 - \frac{1}{6}C_7 - \frac{1}{2}C_8\right),
\end{aligned} \tag{20}
$$

where $\xi_u = V_{ub}^* V_{ud}$, $\xi_t = V_{tb}^* V_{td}$.

Similarly, the decay amplitude for $B_s \to \rho^0 \bar{K}^0$ can be written as

$$
\begin{aligned}
& \mathcal{M}(\rho^0 \bar{K}^0) \\
& = F_{eK}\left[\xi_u\left(C_1 + \frac{1}{3}C_2\right)\right. \\
& \qquad \left. - \xi_t\left(-\frac{1}{3}C_3 - C_4 + \frac{3}{2}C_7 + \frac{1}{2}C_8 + \frac{5}{3}C_9 + C_{10}\right)\right] f_1 \\
& \quad + M_{eK}\left[\xi_u C_2 - \xi_t\left(-C_3 - \frac{3}{2}C_8 + \frac{1}{2}C_9 + \frac{3}{2}C_{10}\right)\right] f_1 \\
& \quad + M_{eK}^{P_1}\xi_t\left(C_5 - \frac{1}{2}C_7\right) f_1 + M_{aK}\xi_t\left(C_3 - \frac{1}{2}C_9\right) f_1 \\
& \quad + M_{aK}^{P_1}\xi_t\left(C_5 - \frac{1}{2}C_7\right) f_1 \\
& \quad + F_{aK}\xi_t\left(\frac{1}{3}C_3 + C_4 - \frac{1}{6}C_9 - \frac{1}{2}C_{10}\right) f_1 \\
& \quad + F_{aK}^{P_2}\xi_t\left(\frac{1}{3}C_5 + C_6 - \frac{1}{6}C_7 - \frac{1}{2}C_8\right) f_1 ,
\end{aligned} \tag{21}
$$

with $f_1 = 1/\sqrt{2}$.

For the decay amplitude of $B_s \to \omega \bar{K}^0$ decay, one can obtain its decay amplitude from (21) by replacing the vector meson ρ with ω, i.e,

$$
f_\rho \to f_\omega\,, \quad f_\rho^T \to f_\omega^T\,, \quad m_\rho \to m_\omega\,. \tag{22}
$$

Note that we have considered the difference in the quark components for the two scalar mesons K^+ and K^0 in the analytic expressions. We denote the corresponding amplitudes for $B_s \to \omega \bar{K}^0$ decay by F'_{eK}, M'_{eK}, $M'^{P_1}_{eK}$, M'_{aK}, $M'^{P_1}_{aK}$, F'_{aK} and $F'^{P_2}_{aK}$, but we do not show explicit expressions of these amplitudes here for the sake of simplicity. The total amplitude finally can be written as

$$
\begin{aligned}
& \mathcal{M}(\omega \bar{K}^0) \\
& = F'_{eK}\left[\xi_u\left(C_1 + \frac{1}{3}C_2\right)\right. \\
& \qquad - \xi_t\left(\frac{7}{3}C_3 + \frac{5}{3}C_4 + 2C_5 + \frac{2}{3}C_6\right. \\
& \qquad \left.\left. + \frac{1}{2}C_7 + \frac{1}{6}C_8 + \frac{1}{3}C_9 - \frac{1}{3}C_{10}\right)\right] f_1 \\
& \quad + M'_{eK}\left[\xi_u(C_2) - \xi_t\left(C_3 + 2C_4 - 2C_6\right.\right. \\
& \qquad \left.\left. - \frac{1}{2}C_8 - \frac{1}{2}C_9 + \frac{1}{2}C_{10}\right)\right] f_1 \\
& \quad - M'^{P_1}_{eK}\xi_t\left(C_5 - \frac{1}{2}C_7\right) f_1 - M'_{aK}\xi_t\left(C_3 - \frac{1}{2}C_9\right) f_1 \\
& \quad - M'^{P_1}_{aK}\xi_t\left(C_5 - \frac{1}{2}C_7\right) f_1 \\
& \quad - F'_{aK}\xi_t\left(\frac{1}{3}C_3 + C_4 - \frac{1}{6}C_9 - \frac{1}{2}C_{10}\right) f_1 \\
& \quad + F'^{P_2}_{aK}\xi_t\left(\frac{1}{3}C_5 + C_6 - \frac{1}{6}C_7 - \frac{1}{2}C_8\right) f_1 ,
\end{aligned} \tag{23}
$$

with $f_1 = 1/\sqrt{2}$.

4 Numerical results

In the numerical calculations we use the following input parameters:

$$
\begin{aligned}
\Lambda_{\overline{\rm MS}}^{(f=4)} &= 250\,{\rm MeV}\,, & f_\rho &= 205\,{\rm MeV}\,, \\
f_\rho^T &= 160\,{\rm MeV}\,, & m_0^K &= 1.6\,{\rm GeV}\,, \\
f_{B_s} &= 236\,{\rm MeV}\,, & f_K &= 160\,{\rm MeV}\,, \\
m_\omega &= 0.782\,{\rm GeV}\,, & f_\omega &= 200\,{\rm MeV}\,, \\
f_\omega^T &= 160\,{\rm MeV}\,, & m_\rho &= 0.770\,{\rm GeV}\,, \\
M_{B_s} &= 5.37\,{\rm GeV}\,, & M_W &= 80.42\,{\rm GeV}\,.
\end{aligned} \tag{24}
$$

The central values of the CKM matrix elements to be used in numerical calculations are [40]

$$
\begin{aligned}
|V_{ud}| &= 0.9745\,, & |V_{ub}| &= 0.0038\,, \\
|V_{tb}| &= 1\,, & |V_{td}| &= 0.0083\,.
\end{aligned} \tag{25}
$$

For the B_s meson wave function, we adopt the model

$$\phi_{B_s}(x,b) = N_{B_s} x^2(1-x)^2 \exp\left[-\frac{M_{B_s}^2 x^2}{2\omega_b^2} - \frac{1}{2}(\omega_b b)^2\right], \tag{26}$$

where ω_b is a free parameter, and we take $\omega_b = 0.5 \pm 0.05\,\text{GeV}$ in numerical calculations, and $N_{B_s} = 65.332$ is the normalization factor for $\omega_b = 0.5$. This is the same wave function as used in [15, 18, 41].

For the light meson wave function, we neglect the b dependent part, which is not important in our numerical analysis. We use the distribution amplitude (DA) of the ρ and ω meson as given in [39]:

$$\phi_{\rho(\omega)}(x) = \frac{3}{\sqrt{6}} f_{\rho(\omega)} x(1-x)\left[1 + 0.18 C_2^{3/2}(2x-1)\right], \tag{27}$$

$$\phi^t_{\rho(\omega)}(x) = \frac{f^T_{\rho(\omega)}}{2\sqrt{6}}\{3(2x-1)^2 + 0.3(2x-1)^2[5(2x-1)^2 - 3] + 0.21[3 - 30(2x-1)^2 + 35(2x-1)^4]\}, \tag{28}$$

$$\phi^s_{\rho(\omega)}(x) = \frac{3}{2\sqrt{6}} f^T_{\rho(\omega)}(1-2x)[1 + 0.76(10x^2 - 10x + 1)], \tag{29}$$

where $C_2^{3/2}(t) = 3(5t^2-1)/2$. For the K meson, we use the same distribution amplitudes ϕ_K^A, ϕ_K^P and ϕ_K^T as used in [20].

From (10), it is straightforward to find the numerical value of the form factor at zero momentum transfer:

$$F_0^{B_s\to K}(q^2=0) = \frac{F_{eK}}{m_{B_s}^2} = 0.28^{+0.05}_{-0.04}, \tag{30}$$

for $\omega_b = 0.50 \pm 0.05\,\text{GeV}$, which agrees well with the value as given in [20, 46, 47].

For $B_s \to \rho(\omega)K$ decays, the decay amplitudes as given in (20), (21) and (23) can be rewritten as

$$\mathcal{M} = V_{ub}^* V_{ud} T - V_{tb}^* V_{td} P = V_{ub}^* V_{ud} T\left[1 + z\mathrm{e}^{\mathrm{i}(\alpha+\delta)}\right], \tag{31}$$

where $\alpha = \arg\left[-\frac{V_{td}V_{tb}^*}{V_{ud}V_{ub}^*}\right]$ is the weak phase (one of the three CKM angles), and δ is the relative strong phase between the tree ("T") and penguin ("P") amplitude, while the term "z" describes the ratio of penguin to tree contributions and is defined as

$$z = \left|\frac{V_{tb}^* V_{td}}{V_{ub}^* V_{ud}}\right|\left|\frac{P}{T}\right|. \tag{32}$$

The ratio z and the strong phase δ can be calculated in the pQCD approach. The CP-averaged branching ratio, consequently, can be defined as

$$\begin{aligned}\text{Br} &= (|\mathcal{M}|^2 + |\overline{\mathcal{M}}|^2)/2 \\ &= \left|V_{ub}V_{ud}^* T\right|^2[1 + 2z\cos\alpha\cos\delta + z^2].\end{aligned} \tag{33}$$

Using the wave functions and the input parameters as specified in previous sections, it is straightforward to calculate the CP-averaged branching ratios for the three decays considered. The numerical results are

$$\text{Br}\big(B_s \to \rho^\pm K^\mp\big) = \big[24.7^{+10.1}_{-6.7}(\omega_b)^{+1.1}_{-1.2}(\alpha)\big] \times 10^{-6}, \tag{34}$$

$$\text{Br}\big(B_s \to \rho^0 \bar{K}^0\big) = \big[1.2^{+0.4}_{-0.2}(\omega_b) \pm 0.1(\alpha)\big] \times 10^{-7}, \tag{35}$$

$$\text{Br}\big(B_s \to \omega \bar{K}^0\big) = \big[1.7^{+0.6}_{-0.3}(\omega_b) \pm 0.02(\alpha)\big] \times 10^{-7}, \tag{36}$$

where the major errors are induced by the uncertainty of $\omega_b = 0.5 \pm 0.05\,\text{GeV}$ and $\alpha = 100^\circ \pm 20^\circ$, respectively.

For comparison, we list the corresponding QCDF predictions for the branching ratios as given in [16]:

$$\text{Br}\big(B_s \to \rho^\pm K^\mp\big) = \big[24.5^{+15.2}_{-12.9}\big] \times 10^{-6}, \tag{37}$$

$$\text{Br}\big(B_s \to \rho^0 \bar{K}^0\big) = \big[6.1^{+12.6}_{-6.0}\big] \times 10^{-7}, \tag{38}$$

$$\text{Br}\big(B_s \to \omega \bar{K}^0\big) = \big[5.1^{+8.3}_{-4.0}\big] \times 10^{-7}, \tag{39}$$

where the individual errors as given in [16] have been added in quadrature. One can see that (a) for $B_s \to \rho^\pm K^\mp$ decay, the theoretical predictions in both QCDF and pQCD approach agree very well; and (b) for $B_s \to (\rho^0, \omega)\bar{K}^0$ decays, however, the central values of the pQCD predictions are smaller than those in the QCDF approach by a factor of 3 to 5, but they are still consistent within one standard deviation, since the theoretical error of QCDF predictions is very large.

Since the contributions from annihilation diagrams are incalculable within the QCDF approach and so can only be estimated using a simple model with the free complex parameters ρ_A and ϕ_A [16] one large theoretical error arises inevitably. In the pQCD factorization approach, however, besides the usual factorizable and non-factorizable diagrams, the annihilation diagrams can also be calculated analytically, and this may provide a large contribution to the branching ratios of the decay modes considered. Furthermore, the non-factorizable and annihilation diagrams also provide the large strong phase required to induce large CP-violating asymmetries for the considered decays (see next subsection for details). Finally, theoretical calculations based on different approaches also provide a means to cross check. This is the reason why we calculate these decays in the pQCD approach and compare our results with those obtained in the QCDF approach. Of course, the differences between the two approaches will be tested in the forthcoming LHC experiments.

In Fig. 2, we show the α and ω_b dependence of the pQCD predictions for the CP-averaged branching ratios of $B_s \to \rho^\pm K^\mp$ decay for $\alpha = [0^\circ, 180^\circ]$ and $\omega_b = 0.5 \pm 0.05\,\text{GeV}$.

It is worth stressing that the pQCD predictions for the branching ratios have a weak dependence on the angle α, but a strong dependence on the parameter ω_b. The ω_b dependence could be fixed by the well measured $B_s \to K$ form factors from the semi-leptonic B_s decays as expected in LHCb experiment. The remaining uncertainties induced by the next-to-leading order α_s QCD corrections and higher twist contributions are not considered here; they need more complicated calculations. The parameter

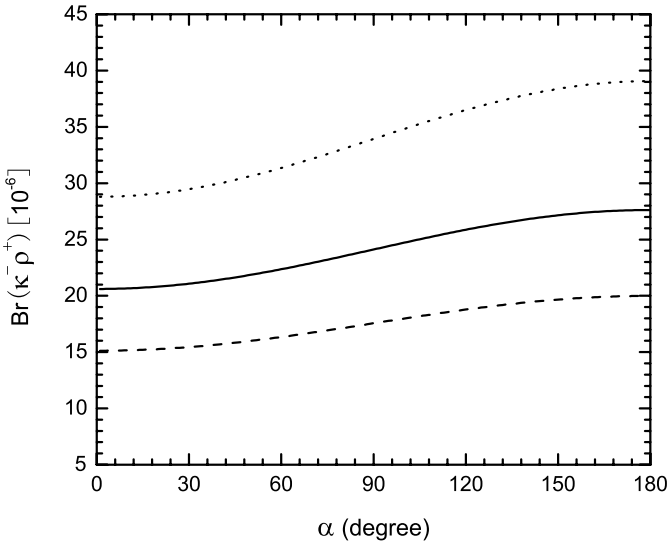

Fig. 2. The branching ratio (in unit of 10^{-6}) of $B_s \to \rho^{\pm}K^{\mp}$ decay for $\omega_b = 0.45$ GeV (*dotted curve*), 0.50 GeV (*solid curve*) and 0.55 GeV (*dashed curve*), as a function of the CKM angle α

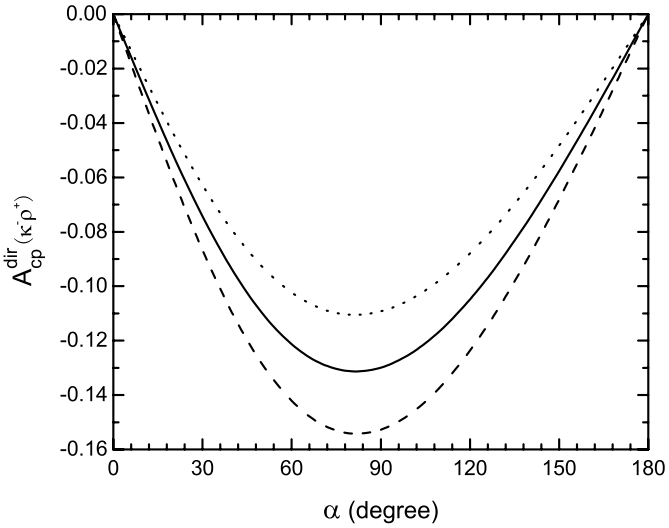

Fig. 3. The α dependence of the direct CP-asymmetries of $B_s \to \rho^{\pm}K^{\mp}$ decay for $\omega_b = 0.45$ GeV (*dotted curve*), 0.50 GeV (*solid curve*) and 0.55 GeV (*dashed curve*)

$m_0^K \approx 1.6$ GeV characterizes the relative size of the twist-3 contribution to the twist-2 contribution. Because of the chiral enhancement of m_0^K, the twist-3 contribution becomes comparable in size with the twist-2 contribution.

Now we turn to the evaluations of the CP-violating asymmetries of $B_s \to \rho(\omega)K$ decays in pQCD approach. For $B_s \to \rho^+K^-$ decay, the direct CP-violating asymmetry $\mathcal{A}_{CP}$ can be defined as

$$\mathcal{A}_{CP}^{\rm dir} = \frac{|\mathcal{M}|^2 - |\overline{\mathcal{M}}|^2}{|\mathcal{M}|^2 + |\overline{\mathcal{M}}|^2} = \frac{-2z\sin\alpha\sin\delta}{1 + 2z\cos\alpha\cos\delta + z^2}\,, \qquad (40)$$

where the ratio z and the strong phase δ have been defined in the previous subsection and are calculable in the pQCD approach.

For $B_s \to \rho^+K^-$ decay, the CP-violating asymmetry is

$$\mathcal{A}_{CP}^{\rm dir}\big(B_s \to \rho^{\pm}K^{\mp}\big) = \big(-12.5^{+2.0}_{-2.2}(\omega_b)^{-0.6}_{+2.0}(\alpha)\big) \times 10^{-2}. \qquad (41)$$

Here two major errors are induced by $\omega_b = 0.50 \pm 0.05$ GeV and $\alpha = 100^\circ \pm 20^\circ$. Although the central values of the pQCD and QCDF prediction, $\mathcal{A}_{CP}^{\rm dir}\big(B_s \to \rho^{\pm}K^{\mp}\big) = (-1.5 \pm 12.2) \times 10^{-2}$ as given in [16] are very different, they are still consistent within one standard deviation, because of the very large error of the QCDF prediction.

In Fig. 3, we show the α and ω_b dependence of the direct CP-violating asymmetries $\mathcal{A}_{CP}^{\rm dir}$ for $B_s \to \rho^{\pm}K^{\mp}$ decay. The possible theoretical errors induced by the uncertainties of other input parameters are usually not large, since both z and δ are stable against their variations. Uncertainties not included here are the next-to-leading order contributions, which may affect the CP-asymmetry strongly [48].

For $B_s \to \rho^{\pm}K^{\mp}$ decay, fortunately, a large CP-asymmetry at the -12% level plus large branching ratios at the 10^{-5} level are measurable in the forthcoming LHC-b experiment. This is indeed good news!

For the pure neutral decays $B_s \to \rho^0\bar{K}^0$ and $\omega\bar{K}^0$, there is both direct and mixing-induced CP-violation. Using (40), we find that

$$\begin{aligned}\mathcal{A}_{CP}^{\rm dir}\big(B_s \to \rho^0\bar{K}^0\big) &= \big(-91.9^{-1.8}_{+8.0}(\omega_b)^{+6.5}_{+4.8}(\alpha)\big) \times 10^{-2},\\ \mathcal{A}_{CP}^{\rm dir}\big(B_s \to \omega\bar{K}^0\big) &= \big(+81.2^{+1.7}_{-5.6}(\omega_b)^{-1.2}_{-8.8}(\alpha)\big) \times 10^{-2},\end{aligned} \qquad (42)$$

for $\omega_b = 0.50 \pm 0.05$ GeV and $\alpha = 100^\circ \pm 20^\circ$. The above pQCD predictions are quite different from those obtained by using the QCDF approach as given in [16]:

$$\begin{aligned}\mathcal{A}_{CP}^{\rm dir}\big(B_s \to \rho^0\bar{K}^0\big) &= \big(24.7^{+58.3}_{-56.8}\big) \times 10^{-2},\\ \mathcal{A}_{CP}^{\rm dir}\big(B_s \to \omega\bar{K}^0\big) &= \big(-43.9^{+69.1}_{-62.1}\big) \times 10^{-2}.\end{aligned} \qquad (43)$$

The reason is the great difference in the source of the strong phases in the two factorization approaches. In the QCDF approach, the strong phase mainly comes from the perturbative charm quark loop diagram, which is α_s suppressed [16]. But the strong phase in the pQCD approach comes mainly from non-factorizable and annihilation type diagrams. It may be difficult to test such differences in the forthcoming LHC experiments because of their small branching ratios at 10^{-7} level.

Following [20], the mixing-induced CP-asymmetry for $B_s \to \rho^0\bar{K}^0$ and $\omega\bar{K}^0$ decays can be defined as

$$\mathcal{A}_{CP}^{\rm mix} = \frac{-2\,{\rm Im}(\lambda_{CP})}{1 + |\lambda_{CP}|^2} = \frac{\sin 2\gamma + 2\,{\rm Re}(x)\sin\gamma}{1 + |x|^2 + 2\,{\rm Re}(x)\cos\gamma}\,, \qquad (44)$$

where $x = \frac{V_{cb}V_{cd}^*}{|V_{ub}V_{ud}^*|}\frac{P}{T+P}$, and the angle γ is one of the three CKM angles. Numerically, the pQCD predictions for the

mixing-induced CP-asymmetry are

$$\begin{aligned}\mathcal{A}_{CP}^{\rm mix}\big(B_s \to \rho^0 \bar{K}^0\big) &= \big(-37^{+22}_{-19}(\omega_b)^{+26}_{+22}(\gamma)\big)\times 10^{-2},\\ \mathcal{A}_{CP}^{\rm mix}\big(B_s \to \omega \bar{K}^0\big) &= \big(-40 \pm 11(\omega_b)^{+19}_{-15}(\gamma)\big)\times 10^{-2},\end{aligned} \tag{45}$$

for $\omega_b = 0.50 \pm 0.05\,\text{GeV}$ and $\gamma = 60^\circ \pm 20^\circ$ (γ is one of the three CKM angles).

5 Conclusion

In this paper, we calculate the branching ratios and CP-violating asymmetries of $B_s \to \rho^\pm K^\mp$, $\rho^0\bar{K}^0$ and $\omega\bar{K}^0$ decays in the pQCD factorization approach.

From our calculations and phenomenological analysis, we found the following results.

- From analytical calculations, the form factor $F^{B_s\to K}(0)$ can be extracted. The pQCD prediction is $F^{B_s\to K}(0) = 0.28^{+0.05}_{-0.04}$ for $\omega_b = 0.50 \pm 0.05\,\text{GeV}$.
- For the CP-averaged branching ratios, the pQCD predictions are

$$\begin{aligned}\text{Br}\big(B_s \to \rho^\pm K^\mp\big) &\approx 24.7\times 10^{-6},\\ \text{Br}\big(B_s \to \rho^0 \bar{K}^0\big) &\approx 1.2\times 10^{-7},\\ \text{Br}\big(B_s \to \omega \bar{K}^0\big) &\approx 1.7\times 10^{-7}.\end{aligned} \tag{46}$$

  The theoretical uncertainties are around thirty to fifty percent.
- For the CP-violating asymmetries, the pQCD predictions are generally large in size. For $B_s \to \rho^\pm K^\mp$ decay, a large CP-asymmetry around -12% plus large branching ratios at 10^{-5} level are measurable in the forthcoming LHC-b experiments.

Acknowledgements. We are very grateful to Cai-Dian Lü, Libo Guo, Hui-Sheng Wang, Xin Liu and Qian-Gui Xu for helpful discussions. This work is partly supported by the National Natural Science Foundation of China under Grant No.10275035 and 10575052, and by the Specialized Research Fund for the Doctoral Program of Higher Education (SRFDP) under Grant No. 20050319008.

Appendix: Related functions

We show here the functions h_i appearing in the expressions of the decay amplitudes in Sect. 3, coming from the Fourier transformations of the function $H^{(0)}$,

$$\begin{aligned}&h_e(x_1,x_3,b_1,b_3)\\ &= K_0(\sqrt{x_1x_3}m_{B_s}b_1)\\ &\quad\times[\theta(b_1-b_3)K_0(\sqrt{x_3}m_{B_s}b_1)I_0(\sqrt{x_3}m_{B_s}b_3)\\ &\qquad+\theta(b_3-b_1)K_0(\sqrt{x_3}m_{B_s}b_3)I_0(\sqrt{x_3}m_{B_s}b_1)]S_t(x_3)\,,\end{aligned} \tag{A.1}$$

$$\begin{aligned}&h_a(x_2,x_3,b_2,b_3)\\ &= K_0(\mathrm{i}\sqrt{x_2x_3}m_{B_s}b_2)\\ &\quad\times[\theta(b_3-b_2)K_0(\mathrm{i}\sqrt{x_3}m_{B_s}b_3)I_0(\mathrm{i}\sqrt{x_3}m_{B_s}b_2)\\ &\qquad+\theta(b_2-b_3)K_0(\mathrm{i}\sqrt{x_3}m_{B_s}b_2)I_0(\mathrm{i}\sqrt{x_3}m_{B_s}b_3)]S_t(x_3)\,,\end{aligned} \tag{A.2}$$

$$\begin{aligned}&h_f(x_1,x_2,x_3,b_1,b_2)\\ &= \{\theta(b_2-b_1)I_0(M_{B_s}\sqrt{x_1x_3}b_1)K_0(M_{B_s}\sqrt{x_1x_3}b_2)\\ &\qquad+(b_1\leftrightarrow b_2)\}\\ &\quad\times\begin{pmatrix}K_0(M_{B_s}F_{(1)}b_2)\,, & \text{for}\quad F^2_{(1)}>0\\ \frac{\pi\mathrm{i}}{2}H_0^{(1)}\big(M_{B_s}\sqrt{|F^2_{(1)}|}b_2\big)\,, & \text{for}\quad F^2_{(1)}<0\end{pmatrix},\end{aligned} \tag{A.3}$$

$$\begin{aligned}&h_f^1(x_1,x_2,x_3,b_1,b_2)\\ &= \{\theta(b_1-b_2)K_0(\mathrm{i}\sqrt{x_2x_3}b_1M_{B_s})I_0(\mathrm{i}\sqrt{x_2x_3}b_2M_{B_s})\\ &\qquad+(b_1\leftrightarrow b_2)\}\\ &\quad\times\begin{pmatrix}K_0(M_{B_s}F_{(2)}b_1)\,, & \text{for}\quad F^2_{(2)}>0\\ \frac{\pi\mathrm{i}}{2}H_0^{(1)}\big(M_{B_s}\sqrt{|F^2_{(2)}|}b_1\big)\,, & \text{for}\quad F^2_{(2)}<0\end{pmatrix},\end{aligned} \tag{A.4}$$

$$\begin{aligned}&h_f^2(x_1,x_2,x_3,b_1,b_2)\\ &= \{\theta(b_1-b_2)K_0(\mathrm{i}\sqrt{x_2x_3}b_1M_{B_s})I_0(\mathrm{i}\sqrt{x_2x_3}b_2M_{B_s})\\ &\qquad+(b_1\leftrightarrow b_2)\}\\ &\quad\times\begin{pmatrix}K_0(M_{B_s}F_{(3)}b_1)\,, & \text{for}\quad F^2_{(3)}>0\\ \frac{\pi\mathrm{i}}{2}H_0^{(1)}\big(M_{B_s}\sqrt{|F^2_{(3)}|}b_1\big)\,, & \text{for}\quad F^2_{(3)}<0\end{pmatrix},\end{aligned} \tag{A.5}$$

where J_0 is the Bessel function, K_0 and I_0 are the modified Bessel functions $K_0(-\mathrm{i}x) = -(\pi/2)Y_0(x) + \mathrm{i}(\pi/2)J_0(x)$; $H_0^{(1)}(z)$ is the Hankel function, $H_0^{(1)}(z) = J_0(z) + \mathrm{i}Y_0(z)$, and the $F_{(j)}$ are defined by

$$\begin{aligned}F^2_{(1)} &= (x_1-x_2)x_3,\\ F^2_{(2)} &= (x_1-x_2)x_3,\\ F^2_{(3)} &= x_1+x_2+x_3-x_1x_3-x_2x_3\,.\end{aligned} \tag{A.6}$$

The threshold resummation form factor $S_t(x_i)$ is adopted from [37, 38]

$$S_t(x) = \frac{2^{1+2c}\Gamma(3/2+c)}{\sqrt{\pi}\Gamma(1+c)}[x(1-x)]^c, \tag{A.7}$$

where the parameter $c = 0.3$.

The Sudakov factors appearing in (10)–(19) are defined as

$$\begin{aligned}S_{ab}(t) &= s\big(x_1m_{B_s}/\sqrt{2},b_1\big)+s\big(x_3m_{B_s}/\sqrt{2},b_3\big)\\ &\quad+s\big((1-x_3)m_{B_s}/\sqrt{2},b_3\big)\\ &\quad-\frac{1}{\beta_1}\left[\ln\frac{\ln(t/\Lambda)}{-\ln(b_1\Lambda)}+\ln\frac{\ln(t/\Lambda)}{-\ln(b_3\Lambda)}\right],\end{aligned} \tag{A.8}$$

$$\begin{aligned}S_{cd}(t) &= s\big(x_1m_{B_s}/\sqrt{2},b_1\big)+s\big(x_2m_{B_s}/\sqrt{2},b_2\big)\\ &\quad+s\big((1-x_2)m_{B_s}/\sqrt{2},b_2\big)+s\big(x_3m_{B_s}/\sqrt{2},b_1\big)\\ &\quad+s\big((1-x_3)m_{B_s}/\sqrt{2},b_1\big)\\ &\quad-\frac{1}{\beta_1}\left[2\ln\frac{\ln(t/\Lambda)}{-\ln(b_1\Lambda)}+\ln\frac{\ln(t/\Lambda)}{-\ln(b_2\Lambda)}\right],\end{aligned} \tag{A.9}$$

$$
\begin{aligned}
S_{ef}(t) &= s\big(x_1 m_{B_s}/\sqrt{2}, b_1\big) + s\big(x_2 m_{B_s}/\sqrt{2}, b_2\big) \\
&\quad + s\big((1-x_2) m_{B_s}/\sqrt{2}, b_2\big) + s\big(x_3 m_{B_s}/\sqrt{2}, b_2\big) \\
&\quad + s\big((1-x_3) m_{B_s}/\sqrt{2}, b_2\big) \\
&\quad - \frac{1}{\beta_1}\left[\ln\frac{\ln(t/\Lambda)}{-\ln(b_1\Lambda)} + 2\ln\frac{\ln(t/\Lambda)}{-\ln(b_2\Lambda)}\right], \qquad \text{(A.10)} \\
S_{gh}(t) &= s\big(x_2 m_{B_s}/\sqrt{2}, b_2\big) + s\big(x_3 m_{B_s}/\sqrt{2}, b_3\big) \\
&\quad + s\big((1-x_2) m_{B_s}/\sqrt{2}, b_2\big) \\
&\quad + s\big((1-x_3) m_{B_s}/\sqrt{2}, b_3\big) \\
&\quad - \frac{1}{\beta_1}\left[\ln\frac{\ln(t/\Lambda)}{-\ln(b_3\Lambda)} + \ln\frac{\ln(t/\Lambda)}{-\ln(b_2\Lambda)}\right], \qquad \text{(A.11)}
\end{aligned}
$$

where the function $s(Q,b)$ is given by [49, 50]

$$
s(Q,b) = \int_{1/b}^{Q} \frac{\mathrm{d}\mu}{\mu}\left[\ln\left(\frac{Q}{\mu}\right) A(\alpha(\bar{\mu})) + B(\alpha_{\rm s}(\bar{\mu}))\right], \qquad \text{(A.12)}
$$

with

$$
\begin{aligned}
A &= C_{\rm F}\frac{\alpha_{\rm s}}{\pi} + \left[\frac{67}{9} - \frac{\pi^2}{3} - \frac{10}{27}n_f + \frac{2}{3}\beta_0 \ln\left(\frac{\mathrm{e}^{\gamma_{\rm E}}}{2}\right)\right]\left(\frac{\alpha_{\rm s}}{\pi}\right)^2, \\
B &= \frac{2}{3}\frac{\alpha_{\rm s}}{\pi}\ln\left(\frac{\mathrm{e}^{2\gamma_E - 1}}{2}\right), \qquad \text{(A.13)}
\end{aligned}
$$

where $\gamma_E = 0.57722\ldots$ is the Euler constant, n_f is the active quark flavor number.

The hard scales t_i in the above equations are chosen as

$$
\begin{aligned}
t_e^1 &= \max(\sqrt{x_3} m_{B_s}, 1/b_1, 1/b_3)\,, \\
t_e^2 &= \max(\sqrt{x_1} m_{B_s}, 1/b_1, 1/b_3)\,, \\
t_e^3 &= \max(\sqrt{x_3} m_{B_s}, 1/b_2, 1/b_3)\,, \\
t_e^4 &= \max(\sqrt{x_2} m_{B_s}, 1/b_2, 1/b_3)\,, \\
t_f &= \max(\sqrt{x_1 x_3} m_{B_s}, \sqrt{x_2 x_3} m_{B_s}, 1/b_1, 1/b_2)\,, \\
t_f^1 &= \max(\sqrt{x_2 x_3} m_{B_s}, 1/b_1, 1/b_2)\,, \\
t_f^2 &= \max(\sqrt{x_1 + x_2 + x_3 - x_1 x_3 - x_2 x_3} m_{B_s}, \\
&\qquad \sqrt{x_2 x_3} m_{B_s}, 1/b_1, 1/b_2)\,. \qquad \text{(A.14)}
\end{aligned}
$$

They are given as the maximum energy scale appearing in each diagram to kill the large logarithmic radiative corrections.

References

1. P. Ball et al., CERN Yellow Report 2000-004 [hep-ph/0003238]
2. S. Stone, talk given at the Aspen Winter Conference, Aspen, Colorado, USA, February, 2006
3. G. Raven, talk given at the Belle–ITEP Meeting on the Future of Heavy Flavour Physics, ITEP Moscow, Russia, July 24–25, 2006
4. T. Ruf, talk given at the XXXIII International Conference on High Energy Physics (ICHEP'06), Moscow, Russia, July 26–August 2, 2006
5. M. Wirbel, B. Stech, M. Bauer, Z. Phys. C **29**, 637 (1985)
6. M. Bauer, B. Stech, M. Wirbel, Z. Phys. C **34**, 103 (1987)
7. A. Ali, G. Kramer, C.D. Lü, Phys. Rev. D **58**, 094009 (1998)
8. A. Ali, G. Kramer, C.D. Lü, Phys. Rev. D **59**, 014005 (1999)
9. Y.-H. Chen, H.Y. Cheng, B. Tseng, K.C. Yang, Phys. Rev. D **60**, 094014 (1999)
10. H.Y. Cheng, K.C. Yang, Phys. Rev. D **62**, 054029 (2000)
11. M. Beneke, G. Buchalla, M. Neubert, C.T. Sachrajda, Phys. Rev. Lett. **83**, 1914 (1999)
12. M. Beneke, G. Buchalla, M. Neubert, C.T. Sachrajda, Nucl. Phys. B **591**, 313 (2000)
13. Y.H. Chen, H.Y. Cheng, B. Tseng, Phys. Rev. D **59**, 074003 (1999)
14. B. Tseng, Phys. Lett. B **446**, 125 (1999)
15. J.F. Sun, G.H. Zhu, D.S. Du, Phys. Rev. D **68**, 054003 (2003)
16. M. Beneke, M. Neubert, Nucl. Phys. B **675**, 333 (2003)
17. D. Zhang, Z.J. Xiao, C.S. Li, Phys. Rev. D **64**, 014014 (2001)
18. Y. Li, C.D. Lü, Z.J. Xiao, X.Q. Yu, Phys. Rev. D **70**, 034009 (2004)
19. X.Q. Yu, Y. Li, C.D. Lü, Phys. Rev. D **73**, 017501 (2006)
20. X.Q. Yu, Y. Li, C.D. Lü, Phys. Rev. D **71**, 074026 (2005)
21. J. Zhu, Y.L. Shen, C.D. Lü, J. Phys. G **32**, 101 (2006)
22. Z.J. Xiao, X. Liu, H.S. Wang, hep-ex/0606177
23. G.P. Lepage, S.J. Brodsky, Phys. Rev. D **22**, 2157 (1980)
24. J. Botts, G. Sterman, Nucl. Phys. B **325**, 62 (1989)
25. H.N. Li, H.L. Yu, Phys. Rev. Lett. **74**, 4388 (1995)
26. H.N. Li, H.L. Yu, Phys. Lett. B **353**, 301 (1995)
27. C.H. Chang, H.N. Li, Phys. Rev. D **55**, 5577 (1997)
28. T.W. Yeh, H.N. Li, Phys. Rev. D **56**, 1615 (1997)
29. Y.-Y. Keum, H.N. Li, A.I. Sanda, Phys. Lett. B **504**, 6 (2001)
30. Y.-Y. Keum, H.N. Li, A.I. Sanda, Phys. Rev. D **63**, 054008 (2001)
31. H.N. Li, Phys. Rev. D **66**, 094010 (2002)
32. H.N. Li, B. Tseng, Phys. Rev. D **57**, 443 (1998)
33. G. Buchalla, A.J. Buras, M.E. Lautenbacher, Rev. Mod. Phys. **68**, 1125 (1996)
34. C.D. Lü, K. Ukai, M.Z. Yang, Phys. Rev. D **63**, 074009 (2001)
35. A.G. Grozin, M. Neubert, Phys. Rev. D **55**, 272 (1997)
36. M. Beneke, T. Feldmann, Nucl. Phys. B **592**, 3 (2001)
37. T. Kurimoto, H.N. Li, A.I. Sanda, Phys. Rev. D **65**, 014007 (2002)
38. C.D. Lu, M.Z. Yang, Eur. Phys. J. C **28**, 515 (2003)
39. P. Ball, V.M. Braun, Y. Koike, K. Tanaka, Nucl. Phys. B **529**, 323 (1998)
40. Particle Data Group, S. Eidelman et al., Phys. Lett. B **592**, 1 (2004)
41. X.Q. Li, G.R. Lu, Y.D. Yang, Phys. Rev. D **68**, 114015 (2003)
42. A. Khodjamirian, T. Mannel, M. Melcher, Phys. Rev. D **70**, 094002 (2004)
43. V.M. Braun, A. Lenz, Phys. Rev. D **70**, 074020 (2004)
44. V.M. Braun, I.E. Filyanov , Z. Phys. C **48**, 239 (1990)
45. P. Ball, J. High Energ. Phys. **01**, 010 (1999)
46. D.S. Du, Z.Z. Xing, Phys. Rev. D **48**, 3400 (1993)
47. D.S. Du, M.Z. Yang, Phys. Lett. B **358**, 123 (1995)
48. H.N. Li, S. Mishima, A.I. Sanda, Phys. Rev. D **72**, 114005 (2005)
49. H.N. Li, B. Melic, Eur. Phys. J. C **11**, 695 (1999)
50. H.N. Li, K. Ukai, Phys. Lett. B **555**, 197 (2003)